# An Ensemble Classification Model to Predict Alzheimer's Incidence as Multiple Classes

**P. Radhika Raju [a,*], A. Ananda Rao [a]**

[a] Department of Computer Science and Engineering, JNTUA Engineering of College, Andhra Pradesh-515002, India
*Corresponding Author Email: radhikaraju.p@gmail.com

**Abstract:** This study introduces an ensemble classification model designed to categorize Alzheimer's disease (AD) into four distinct classes—mild dementia, no dementia, moderate dementia, and very mild dementia—using Magnetic Resonance Imaging (MRI). The proposed model entitled the Ensemble Classification Model to Predict Alzheimer's Incidence as Multiple Classes (PAIMC) that integrates a six-dimensional analysis of MR images, encompassing entropies, Fractal Dimensions, Gray Level Run Length Matrix (GLRLM), Gray Level Co-occurrence Matrix (GLCM), morphological features, and Local Binary Patterns. A four-fold multi-label cross-validation approach was employed on a benchmark dataset to evaluate the model's performance. Quantitative analysis reveals that PAIMC consistently achieves superior Decision Accuracy, F-Score, Specificity, Sensitivity Recall, and Precision metrics compared to existing state-of-the-art models. For instance, PAIMC's Decision Accuracy and Precision outperform the second-best model by a notable margin across all folds. The model also demonstrates a significant improvement in Sensitivity Recall and Specificity, reinforcing its efficacy in the multi-class classification of AD stages. A novel data diversity assessment measure was developed and utilized, further confirming the robustness of the PAIMC model. The results underscore the potential of PAIMC as a highly accurate tool for AD classification in clinical settings.

**Keywords:** Mini Mental State Examination (MMSE), PAIMC, Magnetic Resonance Imaging, Alzheimer's Disease, Mild Cognitive Impairment, Support-Vector-Machine.

## 1. Introduction

Alzheimer's disease (AD) is a neurodegenerative disorder influenced by a combination of environmental and genetic factors, predominantly affecting individuals over 65 years of age. Despite the gradual progression of AD, patients can survive up to nine years post-diagnosis. The Mini Mental-state Examination (MMSE) score is a significant indicator for disease estimation, which decreases as the disease progresses, often leading to Mild Cognitive Impairment (MCI), a precursor to dementia.

There has been no treatment for curing the disease Alzheimer's. When the disease is in advanced phases complications will be such as malnutrition, infection or dehydration happens that result towards death. At the stage of MCI, diagnosis would assist the person for concentrating on health way of life. Effective planning results to be careful about loss of memory. Dementia disorders of adult-onset have been among significant global medical problems in industrialized countries, which have maximal effect on lifestyle of an individual. Moreover, these disorders depict a prominent challenge for community over their upgradation from diagnosis early towards life end as in [1]. Here, statistical studies predicted that every 3 seconds, a novel case of dementia has been increasing all over world. It means nearly patients of 50 million have been suffering from disease [1, 2]. Further, these numbers would increase for every 20 years and probably attain patients of 100 million by the end of the year 2040.

Dementia has been syndrome, which hugely develops in adults. Further, it impacts the functionality of brain, every-day activities and effectiveness of communication as in [1-3]. The disease Alzheimer's depicts prevalent dementia of adult-onset. Some of the contributions have highlighted, where early dementia diagnosis has been resourceful to start treatments & to estimate the disease outcomes however could not provide MCI (Mild-cognitive impairment) does not emerge into dementia overt, while other MCI forms depicts mild AD form as in [4]. Upgraded computer strategies might depict a device for AD diagnosis at an early phase and estimates the prodromal forms evolution of MCI or disease into the dementia. MRI strategies have been becoming associated device for prodromal MCI and AD assessment as in [5]. Some of the contributions depending on comparative analysis of neuroimaging and cognitive testing have been

hypothesized, where AD neuroimaging might be adequate for disease estimation [5, 6]. Also, on other dimension, estimating the dementia with ML (machine-learning) becomes more diffused model in practice clinically [7].

Currently, disease Alzheimer's became common disease of neurodegenerative brain in people elderly. As per published report by International Alzheimer's disease, there are approximately dementia patients of 44 million all over the world, and amount would attain by the year 2030 are 76 million and by the year 2050 are 135 million. From these patients, AD (Alzheimer's disease) patients considered for 50-75% as in characterized through onset insidious and increased episodic memory impairment as in [8, 9]. The MCI has been a circumstance, where individual has been mild however noticeable variations in thinking capabilities. Individuals by MCI were likely for developing AD than the people without them as in [10]. Even though, there were no medications for curing AD, some of the medications is been utilized for delaying some symptoms onset and lower the psychological effect on patients like loss of memory in [11]. Hence, precise AD patient's diagnosis or early stage MCI has been more prominent.

Currently, ML and classification of pattern models have been utilized extensively in computer-aided diagnosis brain system development with neuroimaging like MRI, FMRI (Functional MRI), Diffusion-Tensor-Imaging called DTI as in and PET (Positron-Emission-Tomography) [12-15]. Contributions have exhibited that MRI structural has been prominent standardized modality imaging in practice clinically as in & it has been resourceful for tracing diversified AD clinical stages [16, 17]. Hence, our model has been measured on MRI images structure.

Various features types could be extracted from MRI structure for whole-brain like densities of gray matter or intensities, comparison of group cortical thickness as in, texture-measures as in and morphometry [18-21]. Integration of diversified features types could enhance AD diagnosis accuracy when compared to models that utilize for a individual feature as in [22].

The analysis of texture might examine the subtle variations of body; hence, it could be extensively utilized in diagnosis of AD to extract the features of texture. The work adopted statistical model for differentiating cerebral images of MR patients with amenstic and AD MRI. In projected by, features extracted 336 from GLMC (gray-level co-occurrence matrix) have been utilized for AD categorization [23, 24]. The work [25] utilized discrete transform wavelet for extracting features towards AD diagnosing. Currently, MRI morphometric could be adapted for enhancing diagnosing AD features that is noninvasive, safe & reliable. ROI based analysis measures as well as VBM (voxel-based morphometry) has been utilized extensively for measuring

morphometric variations as in [26]. Specifically, VBM has been hypothesis-free and sensitive in localizing regional variations small-scale in the gray matter as in [18]. Hence, it implemented commonly for studying alternations of gray matter in the AD as in [27]. Moreover, we utilized the integration of analysis of VBM and texture for AD research in this manuscript.

Currently, no cure exists for Alzheimer's disease, and in its advanced stages, complications such as malnutrition, infection, or dehydration can lead to death. Early diagnosis at the MCI stage can facilitate proactive health management and delay memory loss. Dementia, including AD, poses a significant global health challenge, with statistical studies indicating an alarming increase in incidence rates.

Despite advancements in neuroimaging techniques such as MRI, which have become crucial in assessing prodromal MCI and AD, there are significant gaps in the early diagnosis and prognosis of the disease. The limitations of current machine learning (ML) models in clinical practice include a lack of precision in the early stages of AD diagnosis and the inability to differentiate between MCI that progresses to overt dementia and MCI that represents a milder form of AD.

This research addresses these challenges by introducing an enhanced feature selection procedure that integrates covariance and SVM-RFE, aiming to refine the diagnosis and prognosis of Alzheimer's disease using MRI scans. We also incorporate multi-dimensional neuroimaging features to improve the accuracy of AD diagnosis beyond the capabilities of models relying on single-feature analysis. Our model evaluates a combination of VBM and texture analysis for AD assessment, which has been underutilized in previous studies.

Moreover, we tackle the issue of overfitting, common in high-dimensional neuroimaging data, by proposing a novel feature selection algorithm. Our contributions include the application of multiple kernel learning algorithms, which have demonstrated efficacy in AD diagnosis, thus pushing forward the boundaries of computer-aided diagnosis systems in neuroimaging.

This paper presents a comprehensive approach to AD classification, leveraging advanced imaging techniques and ML models to enhance the accuracy and reliability of early-stage AD diagnosis and MCI prognostication, thereby contributing significantly to the field of medical diagnostics in neurodegenerative diseases.

Furthermore, the amount of dimensions of neuroimaging has been more than amount of samples. For solving the over fitting issue, it has been required for the choosing the features. Algorithms related to features selection could be segregated into 3 classes called embedded filters wrappers. For more particular , filter models choose features subset such as PCA [28] in

neuroimaging based classification various features selection models have been projected for instance, univariate models, multi variate, perturbation approach and SVM- RFE is been applied successfully in numerous applications of neuroscience, however it could not have effective performance on analysis of image [28-35]. In this manuscript, we enhance the feature selection procedure through integrating covariance and SVM - RFE. Furthermore, we realized some projected learning algorithms such as multiple kernel learning algorithms [36]. Besides, it exhibits effective performance in diagnosis of Alzheimer's disease [37].

## 2. Review of Related Research

The work [38] recommended a deep learning model besides with clinical information and brain network data like age, gender, as well as ApoE gene of subjects for former Alzheimer's investigation as in [38]. The network of brain has been organized, computing functional links in region of brain by deploying resting-state FMRI data. For generating networks, links have been constructed & were susceptible towards MCI and AD. Dataset has been considered from database ADNI. Classification model comprises of diagnosing early, primarily raw R-FRMI has been carried out as in [38]. Later, the data time-series has been attained and that signifies the levels of blood-oxygen in every brain area and varies a long time. Now, the network of brain has been transformed and built towards time-series data of 90 x 90-matrix correlation. The required auto encoder approach has been utilized that 3-layered approach that provides nervous system intellectual growth then excerpts the attributes of brain-network completely as in [38]. If definite data cases has been considered, cross-verification of k-fold has been significantly implemented for evading complication of over-fitting.

The work [39] projected a model known as multi-stage classifier through utilizing ML algorithms such as NB (Naive Bayes), SVM (Support-vector-machine), and KNN (K-nearest-neighbor) for categorizing among diversified subjects. Moreover, particle-swarm-optimization (PSO) that has been a strategy, which chooses features has been enforced for attaining effective features. Usually, image retrieving procedure needs 2 phases: the initial phase incorporates features generation such that, it generates the image of query and later step associates those features through collected in the database as in [39]. Furthermore, algorithm PSO has been utilized for choosing effective biomarkers, which exhibit MCI or AD considered from ADNI (Alzheimer's-disease: Neuroimaging-Initiative) database. Besides, scans MRI have been preprocessed after considering from database. Selection of feature incorporates thickness & volumetric measurements. Also, lists of optimum features have been attained from algorithm PSO as in [39]. Also, Gaussian NB, KNN, SVM has been utilized for discriminating among subjects. 2-phase classifier has been utilized where, in initial phase

classifier GNB has been utilized for categorizing objects among NC, AD and MCI & in later phases KNN and SVM have been utilized for examining the object depending on initial performance [39]. In this, Image Retrieval based on control has been utilized to retrieve images from database.

The work [40] projected a approach, where longitudinal investigation has been executed on MRI consecutively and has been required for designing and computing disease evolution within time for cause of more accurate-diagnosis. Actual process utilizes those morphological brain anomaly features and longitudinal variance in the MRI & classifier constructed for discriminating among diversified clusters. Brain images of MRI for 6 time-points, which has been for consecutive periods in 6 months, have been considered from database ADNI as in [40].

Later, learning of feature has been carried out by 3D-CNN. Also, CNN has been followed through pooling-layer & possess several approaches to pool like gathering mean-value orelse certain neuron sequence or maximal in this segment. However, to contribute characteristics, this 2 x 2 x 2 convolutional operation has been implemented such that linear integration has been researched for neurons pooling.

Fully connected-layer is having neurons, which generate output for overall neurons in linear integration that have been considered from earlier layer & later has been transferred by non-linearity. Ultimately, for last completely linked, layer softmax has been mainly utilized and later finely tuned for BP (Back-Propagation) for estimating probability class as in [40]. Moreover, outcome of every node changes from 0-1, & overall nodes would be as 1. Ultimately, classification incorporates construction of deep-network incorporating 3D RNN and CNN training model. Later, outcomes of the connective layers have been mapped directly by utilizing function softmax. Initial aspects that have trained by 3 dimensional RNN and CNN network have been established & later only topmost fully aspects connective layer and layer softmax has been utilized to estimate have been adjusted such that longitude and dimensional features have been combined for diversified recognition.

Initially, neuroimaging and MRI offer required data for classification of AD dementia and estimation as in [41]. The models ML, paired with information MRI might offer maximal diagnostic accuracy for ARCD (age-related cognitive-decline) in the subjects of dementia as in [42]. Furthermore, it is been hypothesized that, ML supervised approaches produce features knowledge required for correlating sample data AD as in [43]. Further, it has been stated that, cross-validation couple, logistic regression might augment the AD estimation accuracy by amalgamation of speech as in [44]. The work [45] presents that, on other dimension, support-vectors besides by feature reduction strategies have been capable of categorizing subjects of dementia with

an accuracy of 70%. Current study has been designed for identifying AD depending on MRI findings besides with the utilization of 4 ML approaches like NB, KNN, SVM and NN. 3 individual simulations have been designed for testing the approach, and performance model has been measured separately with specified characteristic information of MRI.

For Alzheimer's disease (MCA-AD), Carmen Jiménez-mesa *et al.,* [46] created the multiclass classification approach. This method maps the chosen features into a multiclass subspace using Partial-Least-Squares after a pairwise t-test, and then uses a one-against-one strategy with error correction output codes for categorization. A multi-class Alzheimer's disease diagnostic system was developed by Weiming Lin and colleagues [47] by utilizing linear discriminant analysis (LDA) to combine data from various modalities.

These diagnostic techniques' accuracy is less than 70%, though.

## 3. Methods and Materials

The process flow of the approach of the proposed model has been discussed in the hierarchy of set of stages such as acquisition of MRIs of the brains of different subjects in the inputs of model, preprocessing, mining of the standard features, detecting optimal features, implementation of classifier using optimal features and performing the learning and testing process. The pictorial representation of the process can be found in Figure 1.

The flow is denoting the training and testing phages of the proposed method. The detailed description of these training and testing phases are explored in following sections:
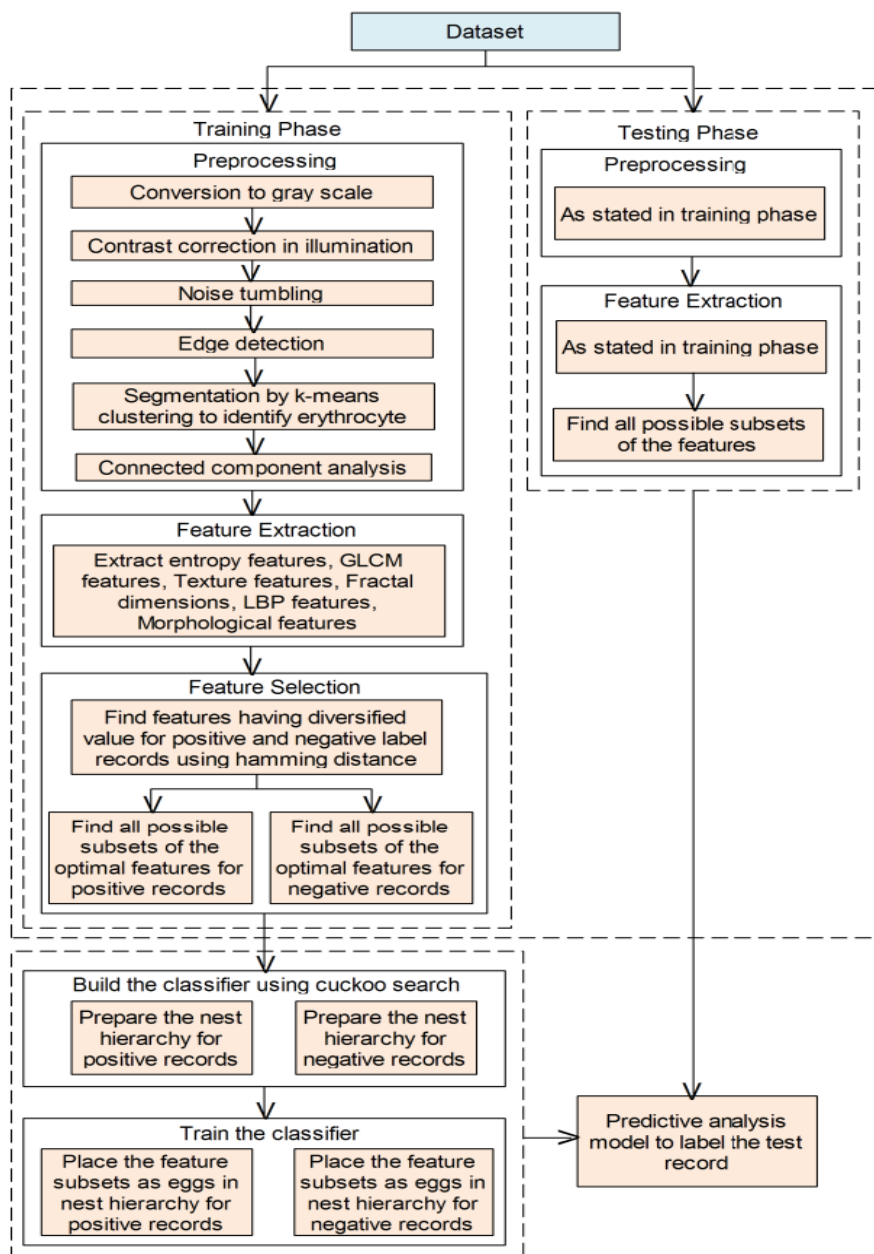


**Figure 1.** The process flow of the PAIMC

## 3.1 Data Set

Dataset consists of two files - Training and Testing both together have a total of 6400 MRI images of human brains each segregated into the severity of Alzheimer's. Magnetic resonance imaging (MRI) of the brain uses magnetic resonance imaging to produce high quality two-dimensional or three-dimensional images of the brain and brainstem without the use of ionizing radiation or radioactive tracers.

## 3.2 Training Phase

Primary effort the first step is preprocessing of the given input images. The preprocessing converts the given images into grey scale images. Then, partitions the resultant grey scale images into 4 groups such that the images labeled as Mild-Demented (MiD), Moderate-Demented (MoD), Non-Demented (NoD), Very-Mild-Demented (vMiD). These images of four classes are further given as input to training phase. The next step of the proposal performs the feature extraction process. Here it extracts the entropy, GLSM, texture, fractal dimensions, LBP, and morphological features. Then the proposal discovers the optimal features, in this segment find the features having diversified value for four classes records using diversity assessment metric(s). A feature is said to be optimal, if the feature values of the corresponding feature under four classes MiD, MoD, NoD, and vMiD are distinct. Further, it performs predictive analysis for discovering the Incidence of the Alzheimer's and it's class for the specified test record. In the below description, for the flow diagram, each block is described. Training phase consists of preprocessing, Feature extraction, Feature selection and labeling and feature classification.

### 3.2.1. Pre-processing

The basic objective of this step is to improve the classification accuracy of MRIs of the brains of different subjects by removing noise, eliminating artefacts which are incorporated during slide preparation and imaging. The main operations used to perform pre-processing are RGB to grey conversion, contrast and brightness improvement, noise removal.

The image preprocessing includes the following tasks:

(i) Removes the MRI images that are not competent to collect the features or not having any of the labels representing the classes MiD, MoD, NoD, and vMiD .

(ii) Performs the image processing that converts the given Magnetic resonance imaging to grey scale format.

(iii) Partitions the given records in to four classes having records labeled as MiD, MoD, NoD, and vMiD in respective order.

### 3.2.1.1 RGB to Grey Conversion

The RGB to grey-scale conversion is the optional step in preprocessing which converts acquired RGB Magnetic resonance imaging of the brains of different subjects into grey scale images by using Principle Component Analysis (PCA). It is a standard linear technique, which reduces the dimensions of 3-channel RGB Magnetic resonance imaging data (if exists) by transforming it into a single channel data. By the use of "Linear Least Square" method, the highest contrast in greyscale could be developed. The color coordinates of RGB are utilized for evaluating the RBC primary color axis and suitable regression line could be formed through a PCA-regression, which lessens distance among axis line and point, which are impacted by parasite effected image cell in regression-space. The input RGB image and output grey-scale images are represented in Figure 2 (a) and Figure 2 (b) respectively. Hence, PCA is an effective method for converting the Magnetic resonance imaging of RGB into greyscale.

The variation angles are represented as g, b and r, are obtained first, then their cosine values are computed and their first and consecutively, here, into grey-scale values. Eq 1, is used for collecting regression weights.

$$\Lambda(xw, yw, zw) = \frac{1}{\sqrt{xw^2 + yw^2 + zw^2}} \sum_{i=0}^{|Pc|} (xwr_k + ywg_k + zwb_k) \quad ...(Eq\ 1)$$

Where $xw, yw, zw$ are the minimum weights assigned to $r, g, b$ respectively.

$|Pc|$ is the pixel count of the image

$vr_k, vg_k, vb_k$ indicates the values of red, green, and blue components for $k^{th}$ pixel.

$$agr(xw, yw, zw) = \sum_{k=0}^{|P_{ix}|} \big((xw * vr_k) + (yw * vg_k) + (zw * vb_k)\big) \text{ (a)}$$

$$sqrt(xw, yw, zw) = \sqrt{(xw)^2 + (yw)^2 + (zw)^2} \qquad \text{(b)}$$

$$\Lambda(xw, yw, zw) = agr(xw, yw, zw) * sqrt(xw, yw, zw)^{-1}$$

### 3.2.1.2. Contrast correction in illumination

Grayscale images can have their contrast improved by applying gamma equalization. Image brightness is managed by gamma correction. Finding the ideal gamma value will improve the quality of the image. The image's contrast can be significantly improved by precisely estimating this value. There is a 0.5 gamma value.

Magnetic resonance imaging poor illumination is featured to a diverse range of circumstances.

Nevertheless, detecting the demented Magnetic Resonance Imaging, which are continuing in dull contrast, could be the important confine. Therefore, the importance of enhancing the levels of contrast is the main step in the segmentation procedure.
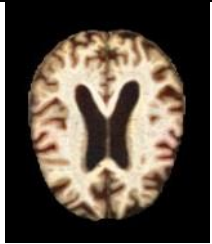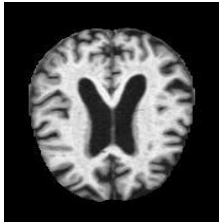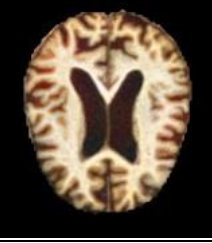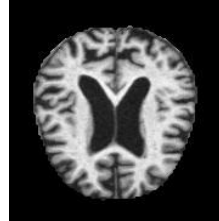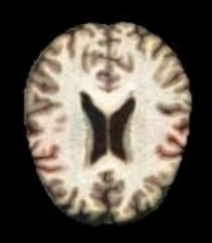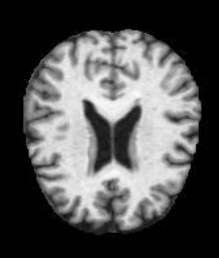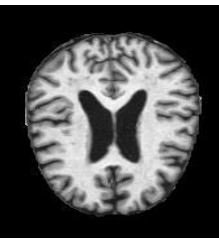
| Class⇓ | RGB Image⇓ | Greyscale Image⇓ |
|---|---|---|
| **Mild demented (MiD)** | | |
| **Moderate Demented (MoD)** | | |
| **No Demented (NoD)** | | |
| **Very Mild Demented (vMiD)** | | |

**Figure 2.** RGB to Grey conversion outcomes

For enhancing the image of grey scale contrast level $b(\overline{m},\overline{n})$ the method termed as GE (gamma equalization) [48], [49] is modified as represented in below equation (see Eq 2):

$$b(\overline{m},\overline{n}) = \gamma\overline{mn}\left|\frac{(\gamma(\overline{m},\overline{n})-\gamma\overline{mn}^{\tau}{}_{min})}{(\gamma\overline{mnmn}^{\tau}{}_{min_{max}}||)}\right|_{max} \quad .(Eq\ 2)$$

Under the threshold levels of gamma is 0.5, the contrast image aimed at greyscale input is depicted in Figure 3.

### 3.2.1.3 Noise Tumbling

The Noise patters of MRIs of the brains of different subjects are removed by the median filter which is in the form of impulse noise by preserving edges and without blurring. Other common types of noise are Pepper & Salt, and splendid imposed patterns affect the MIBS are shown in Figure 4.

### 3.2.1.4 Detecting the Pattern Noise Spectral Peaks

This section explores about the pattern noise spectral peaks. Impulse noise from Fourier amplitude spectrum can be detected by median filter. The distinct filtering procedure is implemented towards any noise from the "Fourier amplitude spectrum" in specified image utilizing (Eq 3).

$$L(sa,sb) = \sum_{\overline{m}=0}^{S_1-1}\sum_{\overline{n}=0}^{R_1-1}\left(l(\overline{m},\overline{n})\gamma^{2\pi\left((sa\overline{m}/R_1)+((sb\overline{n})/S_1)\right)}\right) \quad (Eq\ 3)$$

The notation $l(\overline{m},\overline{n})$ denotes the image size $R_1 \times S_1$ . The spectral amplitude $(sa,sb)^{th}$ coefficients $L(sa,sb)$.

The peaks could be seen as optimistic spots in the spectral amplitude, identical to the impulses in visual

Circumstances. Further phase performs the detection of spectral peak in "Fourier amplitude spectrum".
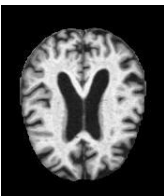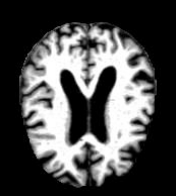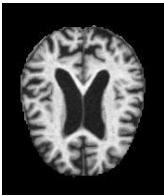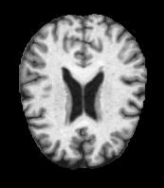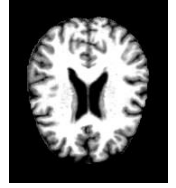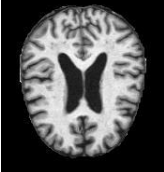
| Label | Original | Contrast Adjusted Gamma Equalization output image($\tau = 0.5$) |
|-------|----------|------------------------------------------------|
| MiD |  |  |
| MoD |  |  |
| NoD |  |  |
| vMiD |  |  |

**Figure 3.** Imagery of Gamma Equalization procedure
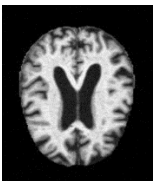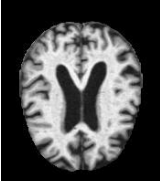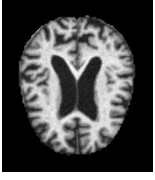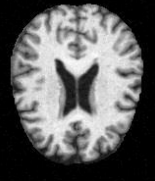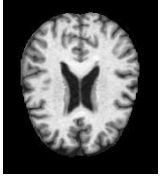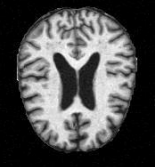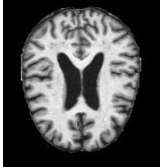
| Class⇓ | Image with noise⇓ | filtered Image⇓ |
|--------|-------------------|-----------------|
| **Mild demented (MiD)** |  |  |
| **Moderate Demented (MoD)** |  |  |
| **No Demented (NoD)** |  |  |
| **Very Mild Demented (vMiD)** |  |  |

**Figure 4.** Gaussian and Median Filtering

| Label | Contrast adjusted Image | Edge Detected using canny spatial high pass filtering |
|---|---|---|
| MiD |  |  |
| MoD |  |  |
| NoD |  |  |
| vMiD |  |  |

**Figure 5.** Edge identification using Canny Edge detection method

### 3.2.1.5 Edge detection

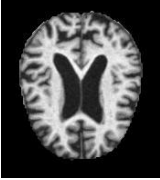Magnetic Resonance Imaging edges are determined by using canny spatial high pass filtering. Canny edge detector is based on first derivative coupled with noise cleaning and retains the continuous borders in an effective way.

As Magnetic Resonance Image affected area appears dark, the borders & edges associated with that dark area are highlighted in Figure 5

### 3.2.1.6 Morphological operations

The Magnetic Resonance Imaging comprise covered areas and eradication of such areas performed by using "morphological binary destruction operation" is explored in this section.

Further, demented Magnetic Resonance Imaging in clustering procedure contains covered region suspended on the demented-Magnetic Resonance Imaging & such excess area or regions requisite to be eradicated. Such a procedure can be performed by concentrating on the "morphological binary destruction operation [49]". Moreover, the $s(\overline{m},\overline{n})$ structuring element is utilized for destructing binary image $b(\overline{m},\overline{n})$, which delivers a resulting binary image $r(\overline{m},\overline{n})$. In (Eq 4), the destruction is conducted as discussed in the following.

$$r(\overline{m},\overline{n}) = \left\{ b(\overline{m},\overline{n}) \wedge b(\overline{m}^1,\overline{n}^1) \exists b(\overline{m}^1,\overline{n}^1) \in s(\overline{m},\overline{n}) \right\} \quad \text{(Eq 4)}$$

For detecting the STREL optimal size, the tests are carried out on $3 \times 3, 5 \times 5$ and $7 \times 7$ STREL square particles & it is vital that $3 \times 3$ are optimal.

## 3.3 Features Extraction

This section covers the process of extracting features from grayscale images to differentiate between demented and non-demented magnetic resonance imaging. Among the characteristic values that need to be determined in this critical step are entropy, texture measures, fractal dimensions, Local Binary Patterns (LBP), morphological attributes, and Gray Level Co-occurrence Matrix (GLCM). Conditions like malaria can be distinguished by morphological and textural characteristics. The morphology, texture, and specific intensity features of an MRI reveal changes caused by malaria parasites. 51 features are used in our analysis: 6 LBP-related, 1 fractal dimension, 5 entropy-based, 19 GLCM-derived, 11 texture-specific, and 9 morphological.

### 3.3.1 Entropy Features

Entropy measures randomness to characterize the textural properties of images. High entropy is indicated by uniform co-occurrence matrix entries. By reflecting texture image uncertainty, entropy helps MRI differentiate between normal and demented states. Five

entropy measures are evaluated in sources [50] and [51].

### 3.3.2 GLCM Features

Through capturing the frequency of co-occurring pixel values at a given distance and direction, the GLCM displays variations in intensity. Contrast, correlation, and energy are among the nineteen GLCM features that are related to information and entropy variance. These features are important for texture analysis, as stated in references [52] to [54].

### 3.3.3. GLRLM Features

To assess textural patterns, the Grey Level Run Length Matrix (GLRLM) quantifies the runs of pixels with the same grey level in a given direction. To comprehend the granular structure of the grey-scale image, the GLRLM takes into account runs of pixels with uniform grey levels. Eleven texture features are produced by this matrix, ranging from SRE and LRE [54-56].

### 3.3.4 Fractal Dimensions

Fractal dimensions measure image surface roughness. In order to identify textural differences on demented MRIs, the fractal dimension method transforms a 2D image into a 3D structure. The box counting method is one of the fractal analysis algorithms used to identify these textural variations [57-59].

### 3.3.5 Local Binary Patterns

LBP is used in feature extraction to combine structural and statistical texture assessment with local image contrasts. In LBP, capturing texture through textons, circular neighborhoods and bilinear interpolation are used. [60, 61] discuss Volume-LBP computation and Local Phase Quantization (LPQ).

The number of pixels in an MRI image, I, within a radius R is known as P_ix in mathematics. To find a binary value, the central pixel, p_c, is compared to each of its surrounding pixels, p_i.

### 3.3.6 Morphological Features

Last morphological features analysis looks at the shape of the MRI. Examined are nine features, including invariant moments that aid in the identification of MRI anomalies. These features are crucial for differentiating demented MRIs from non-demented ones in terms of size and shape, according to [49-63].

## 3.4 Feature Selection

In this step, features are selected with the help of distribution diversity assessment method call t-test. The T-test, which is Conventional approach, has used to scale the diversity of the feature vectors$fv_+^i, fv_-^i$. In lines with the advocated efficacy of T-test [64] for assessing the diversity, depicting the values of distinct sets with similar distribution, in terms of its divergent or being variant.

In [65-66], the authors of the studies have discussed the scope and equation of t-test for verifying the diversity among the features to be used with distinct labelling. The (Eq5) mentioned below is applied for the assessment.

$$t - score = \frac{(Mfv_+^i - Mfv_-^i)}{\sqrt{\frac{\sum_{j=1}^{|fv_+^i|}\left(e_i - Mfv_+^i\right)^2}{|fv_+^i|-1} + \frac{\sum_{j=1}^{|fv_-^i|}\left(e_j - Mfv_-^i\right)^2}{|fv_-^i|-1}}} \quad \text{(Eq 5)}$$

- The notations$Mfv_+^i, Mfv_-^i$ signifies mean of the feature vectors $fv_+^i, fv_-^i$ in respective order. These feature vectors signify the probable value of features of positive and negative labels under one of the available dimensions.

The notations$e_i, e_j$indicate the values imperative in the feature vectors $fv_+^i, fv_-^i$ of relevant sizes$|fv_+^i|, |fv_-^i|$.

The test refers to the outcome in terms of understanding the mean difference and the square root values pertaining to the cumulative of mean square distances. As discussed in [67], [68], the p-value for the t-table indicates potential values, and across the vectors the nature and feature for the vectors are imperative. Low probability in terms of p-value refers to the conditions wherein the two vectors are distinct, and it indicates the features for the vectors as potentially optimum.

## 3.5 Ensemble Classification

Classifier ensemble is performed using the following process. At every positive label cluster$Cl_{+ve}^i$, identify the negative label cluster $Cl_{-ve}^j$ wherein the features quality dimensions are matching to higher proposition. Random forest has to be built from both clusters, so that every dimension depicts the classifier, where each classifier divides further as per the information gain perceived from optimal features patterns of corresponding dimension. Resemblance amongst positive and negative label clusters $Cl_{+ve}^i, Cl_{-ve}^j$ is predicted by any measures of similarity such as Jaccard similarity [69-71] which implemented on every dimension feature. Also, more appropriate features patterns of each corresponding cluster$Cl_{+ve}^i, Cl_{-ve}^j$ have been determined and portrayed below:

Optimum features integral to the positive and negative label clusters $Cl_{+ve}^i, Cl_{-ve}^j$ available has to garner unique set which is more significant to determine cumulative subsets of count $2^n$ -1. Representation n indicates the unique set of cardinalities$v^{dm}$.

Also, the subsets derived from vector $v^{dm}$ is transpired as a set$P_{dm}$, which is used for developing

appropriate random forest classifier which constitutes the clusters $Cl^i_{+ve}, Cl^j_{-ve}$. In furtherance, procedure traces the pattern information using the following steps.

Procedure for detection of the pattern information gain $\{p \exists p \in P_{dm}\{\}\}$ is profoundly associated to the conditions of positive and negative clusters $Cl^i_{+ve}, Cl^j_{-ve}$ in the following way:

Entropy $entr^j_i$ refers obscurity in threshold amongst clusters test records $Cl^i_{+ve}, Cl^j_{-ve}$ constituting positive and negative class test records in an order been assessed and stated in [72-74], wherein it explored in (Eq 6).

$$ entr^j_i = -\left( \frac{\frac{|Cl^i_{+ve}|}{|Cl^i_{+ve}|+|Cl^j_{-ve}|} log_2\left(\frac{|Cl^i_{+ve}|}{|Cl^i_{+ve}|+|Cl^j_{-ve}|}\right) +}{\frac{|Cl^j_{-ve}|}{|Cl^i_{+ve}|+|Cl^j_{-ve}|} log_2\left(\frac{|Cl^j_{-ve}|}{|Cl^i_{+ve}|+|Cl^j_{-ve}|}\right)} \right) \quad \text{(Eq 6)} $$

$\forall^{|P^{k=1}_{dm}|} \{p_k \exists p_k \in P_{dm}\}$ For each pattern Begin,

When a probability of pattern $P$ is zero for either of the clusters $Cl^i_{+ve}, Cl^j_{-ve}$ representing labels positive and negative in respective order, then the entropy of the pattern $P$ is zero (0). Hence, each of the definite pattern shall be distinct to both labels positive and negative.

In the absence of such conditions, the entropy patterns are assessed in terms of positive and negative labels using the Eq 7 depicted below.

$$ entr(p) = -\left( \frac{\frac{\sum^{|Cl^i_{+ve}|}_{m=1}\{1 \exists p \in rs_m \wedge rs_m \in Cl^i_{+ve}\}}{|Cl^i_{+ve}|} log_2 \frac{\sum^{|Cl^i_{+ve}|}_{m=1}\{1 \exists p \in rs_m \wedge rs_m \in Cl^i_{+ve}\}}{|Cl^i_{+ve}|} +}{\frac{\sum^{|Cl^j_{-ve}|}_{n=1}\{1 \exists p \in rs_n \wedge rs_n \in Cl^j_{-ve}\}}{|Cl^j_{-ve}|} log_2 \frac{\sum^{|Cl^j_{-ve}|}_{n=1}\{1 \exists p \in rs_n \wedge rs_n \in Cl^j_{-ve}\}}{|Cl^j_{-ve}|}} \right) $$

$$ \text{(Eq 7)} $$

// the entropy of the pattern

End Also, information gain $infG(p)$ of pattern $p_k$ regarding cluster $Cl^i_{+ve}, Cl^j_{-ve}$ is assessed in the following,

| $infG(p_k)$ $= entr^j_i$ $- entr(p_k)$ | // the difference between the entropy of patterns and it's corresponding dimension $dm$ |
|---|---|
| | End |

### 3.5.1 Information Gain based Feature Hierarchy

Patterns of the features of the dimension $dm$ signified with the notation $P_{dm}$. The patterns stated by notation $P_{dm}$ shall be partitioned as sets $P^{o^{\pm ve}_{dm}}_{dm}$. Set $P^o_{dm}$ constitutes patterns towards reducing sequence size of their information-gain, constitute entropy 0. Set $P^{\pm ve}_{dm}$ constitutes patterns for reducing sequence of their information-gain, where in entropy with more than 0 and is used for identifying classifier hierarchy. The fundamental pattern of information gain order is based on the max to min form which is placed in

distinct kind of classifier hierarchy pattern discussed below.

Every pattern $\{p_i \exists p_i \in P^{\pm ve}_{dm}\{\}\}$ of positive or negative label set $P^{\pm ve}_{dm}$ wherein higher or alike information gain compared to the pattern $P_i$ information shall be maintained at the hierarchy level. Higher or similar information gain in comparison with pattern information gain is managed to the hierarchy.

Also, the patterns are pruned and managed to its hierarchy levels, and such processes are repeated in terms of addressing the levels of remaining patterns over the classifier hierarchy. Further, the patterns of the leftover set $P^o_{dm}$ shall be placed as leaves in classifier hierarchy.

Post observation of the patterns in classifier hierarchy, nodes in the levels of hierarchy are mapped to the child nodes at predecessor levels of the nodes, and the mapping could be to one or more nodes at the predecessor levels.

Also, at every cluster level pair $Cl^i_{+ve}, Cl^j_{-ve}$, the random forest needs has to be integral in terms of random forest ensemble classifier which can be significant for distinct features as classifiers, and the conditions as discussed below.

### 3.5.2 Ensemble Learning

Random Forest $tr$ is constructed for every pair of clusters both positive and negative $Cl^i_{+ve}, Cl^j_{-ve}$ respectively.

The patterns discovered in terms of appropriate features wherein it placed in distinct hierarchy levels in lines with information gain.

### 3.5.2.1 The fitness function of the ensemble classification

To a chosen specified test record $rs$ predicting class label are detailed below,

In the fundamental stage, the pre-processing is performed, and it gathers the features.

The primary stage performs pre-processing and gathers the features.

It denotes the cumulative feature subsets that are associated to the conditions of $dm$ attained from the test record $rs$

For every Classifier $\{cl \exists cl \in Cl\}$ parallel,

$\forall^{i=1}_{|Cl|} \{cl_i \exists cl_i \in Cl\}$ Begin, //For each classifier $cl_i$ find the fitness of the features,

- Count $ptc^{MiD,MoD,NoD,vMiD}_{cl_i}$ the possible paths from root to leaf nodes

- Out of all possible paths $ptc_{cl_i}^{MiD,MoD,orvMiD}$, count the paths signifying $MiD, MoD, NoD, and vMiD$ labels

- test record that denoted as $ptc_{MiD,MoD,orvMiD}^{cl_i}$

- Out of all possible paths $ptc_{NoD}^{cl_i}$, count the paths signifying NoD label

- test record that denoted as $ptc_{NoD}^{cl_i}$

- Determine $MiD, MoD, orvMiD$ path probability $pro_{MiD,MoD,orvMiD}^{cl_i}$ as follows: Eq 8

$$pro_{MiD,MoD,orvMiD}^{cl_i} = \frac{ptc_{MiD,MoD,orvMiD}^{dm_k}}{\sum_{i=1}^{|Cl|} ptc_{cl_i}^{MiD,MoD,orvMiD}} \quad \text{(Eq 8)}$$

*//ratio of paths $ptc_{MiD,MoD,orvMiD}^{cl_i}$ those routing towards $MiD, MoD, NoD, and vMiD$ test record against total number of paths $ptc_{cl_i}^{MiD,MoD,NoD,orvMiD}$*

- Determine the negative path probability $pro_{NoD}^{cl_i}$ as follows: Eq 9

$$pro_{NoD}^{cl_i} = \frac{ptc_{NoD}^{cl_i}}{\sum_{i=1}^{|Cl|} ptc_{cl_i}^{NoD}} \quad \text{(Eq 9)}$$

*//ratio of paths $ptc_{NoD}^{cl_i}$ those routing towards negative test record against total number of paths*

- Determining the feature entropy $entr_{cl_i}^{MiD,MoD,orvMiD}$ format of classifier $tr$ as exhibited in (Eq 10):

$$entr_{cl_i}^{MiD,MoD,orvMiD} = -(pro_{MiD,MoD,orvMiD}^{cl_i} log_2(pro_{MiD,MoD,orvMiD}^{cl_i}) + pro_{NoD}^{cl_i} log_2(pro_{NoD}^{cl_i})) \quad \text{(Eq 10)}$$

- Executing the search must be managed for branch referring to the specified feature dim format in terms of potential paths based on root having mapped leaf.

- Executing the search on branch portraying the stated feature dimension for ascertaining the probable paths between root nodes to leaf nodes.

- Executing the label's $MiD, MoD, NoD, and vMiD$ paths count of mapping the $MiD, MoD, NoD, and vMiD$ labels test record as $ptc_{MiD}, ptc_{MoD}, and ptc_{vMiD}$

- Executing the path probability $pro_{MiD}^{r}, pro_{MoD}^{r}, pro_{vMiD}^{r}$ for constituting leaf nodes, wherein in labels are denoted as demented as shown in (Eq 11).

$$pro_{MiD,MoD,orvMiD}^{r} = \frac{ptc_{MiD,MoD,orvMiD}^{r}}{\sum_{i=1}^{|Cl|}(ptc_{MiD,MoD,orvMiD}^{cl_i})} \quad \text{(Eq 11)}$$

- Tracing the paths count resulting in attaining leaf node indicating the negative label test record as $ptc_{MiD}, ptc_{MoD}, and ptc_{vMiD}$

- Tracing the path possibility $ptc_{MiD}^{r}, ptc_{MoD}^{r}, and ptc_{vMiD}^{r}$ to attain leaf nodes termed for NoD label as shown in following Eq 12.

$$pro_{NoD}^{r} = \frac{ptc_{Nod}^{r}}{\sum_{i=1}^{|Cl|}\{ptc_{NoD}^{cl_i}\}} \quad \text{(Eq 12)}$$

- Tracing entropy $entr_{rs}^{dm}$ of chosen test record $rs$ wherein it leads to classifier $tr$ from following in (Eq 13).

$$entr_{MiD,MoD,orvMiD}^{r} = -(pro_{MiD,MoD,orvMiD}^{r} log_2(pro_{MiD,MoD,orvMiD}^{r}) + pro_{MiD,MoD,orvMiD}^{r} log_2(pro_{MiD,MoD,orvMiD}^{r}) + pro_{NoD}^{r} log_2(pro_{NoD}^{r}))$$

$$\text{(Eq 13)}$$

The entropy $entr_r^{cl_i}$ set to be 0, if and only if one among the counters $ptc_{MiD}^{r}, ptc_{MoD}^{r}, and ptc_{vMiD}^{r}$ is 0,

Assessing information gain $infG_r^{cl_i}$ toward features of labels and classifier $cl_i$ under stated classifier $cl_i$ as follows Eq 14

$$infG_{MiD,MoD,orvMiD}^{cl_i} = entr_{cl_i}^{MiD,MoD,orvMiD} - entr_r^{MiD,MoD,orvMiD}$$

$$\text{(Eq 14)}$$

If the information gain $infG_{MiD,MoD,orvMiD}^{cl_i}$ towards test record $r$ is identical to dimension entropy $entr_{tr}^{dm_k}$ of the corresponding classifier $tr$,

If probability of the path $pro_{MiD,MoD,orvMiD}^{r}$ of the one of the demented $MiD, MoD, orvMiD$ leaf nodes and root node of the corresponding classifier $cl$ exists in the context of test record $r$, the demented $MiD, MoD, orvMiD$ fitness of the test record $r$ shall be one, and the negative fitness of the test record $r$ shall be zero. Else if, positive probability of the path $pro_{MiD,MoD,orvMiD}^{r}$ is zero, the negative fitness of the corresponding $r$ shall be one.

Otherwise, if the information gain $infG_{cl_i}^{MiD,MoD,orvMiD}$ of the test record $rs$ is small that compared to Label $MiD, MoD, orvMiD$ entropy $entr_{cl_i}^{MiD,MoD,orvMiD}$ of the classifier $cl_i$, then the fitness of the corresponding test record $r$ fitness of both labels positive and negative are $\frac{pro_{MiD,MoD,orvMiD}^{r}}{(pro_{MiD,MoD,orvMiD}^{r}+pro_{NoD}^{r})}, \frac{pro_{NoD}^{r}}{(pro_{MiD,MoD,orvMiD}^{r}+pro_{NoD}^{r})}$ in respective order.

Total fitness feature format level for the specified test record $rs$ towards handling the negative and positive labels, wherein in inferior bound fitness at specific label results in feature format, and accordingly the random forest classifiers are developed to execute ensemble-classification. The outcome from the process remains an absolute variance for average fitness and resulting label of MSE.

Also, the label shall be categorized to chosen test record based on the cumulative fitness perceived in terms of handling Mild Dement, Moderate Dement, very Mild Dement and No Dement labels result in format feature aggregation. The label is allocated to specific set of test records wherein the higher value of aggregate is integral to managing the fitness of feature format.

## 4. Experimental Study

In this empirical study, the projected approach Predict Alzheimer's Incidence as Multiple Classes (PAIMC) performance has been compared with other existing approaches MCA-AD and ADMD have been measured by utilizing metrics called accuracy, sensitivity, precision and F-measure over the 4 folds [46, 47].
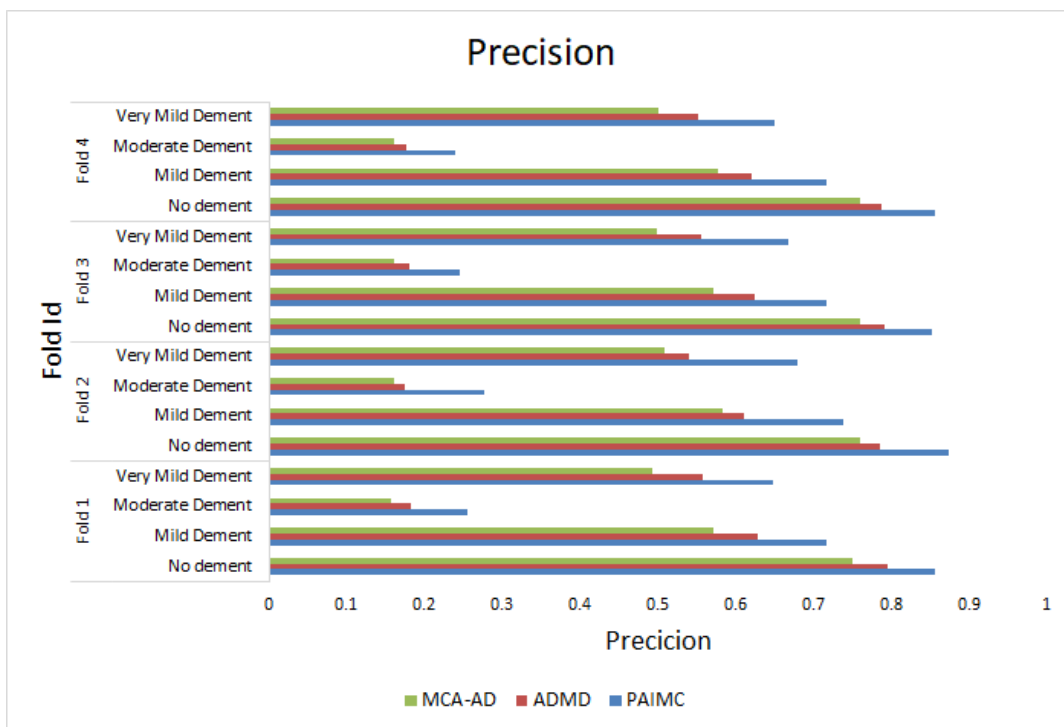


**Figure 6.** Graphical representation of comparison of proposed model PAIMC and contemporary model's ADMD and MCA-AD in terms of metric precision over four folds.
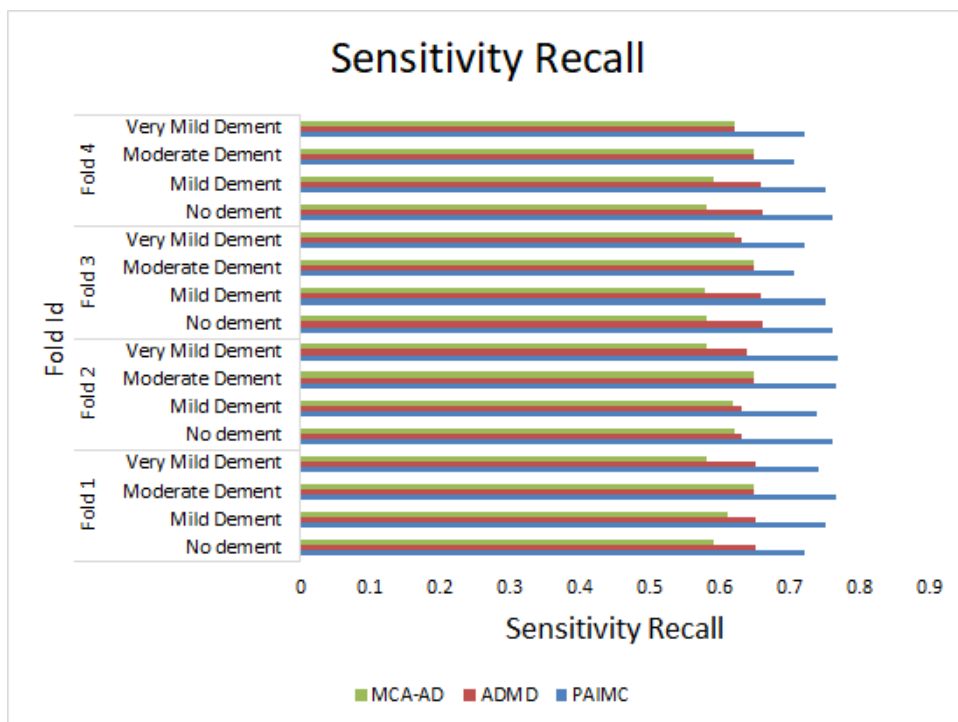


**Figure 7.** Graph showing metric sensitivity of PAIMC compared to ADMD and MCA-AD with regard to four-fold cross validation.
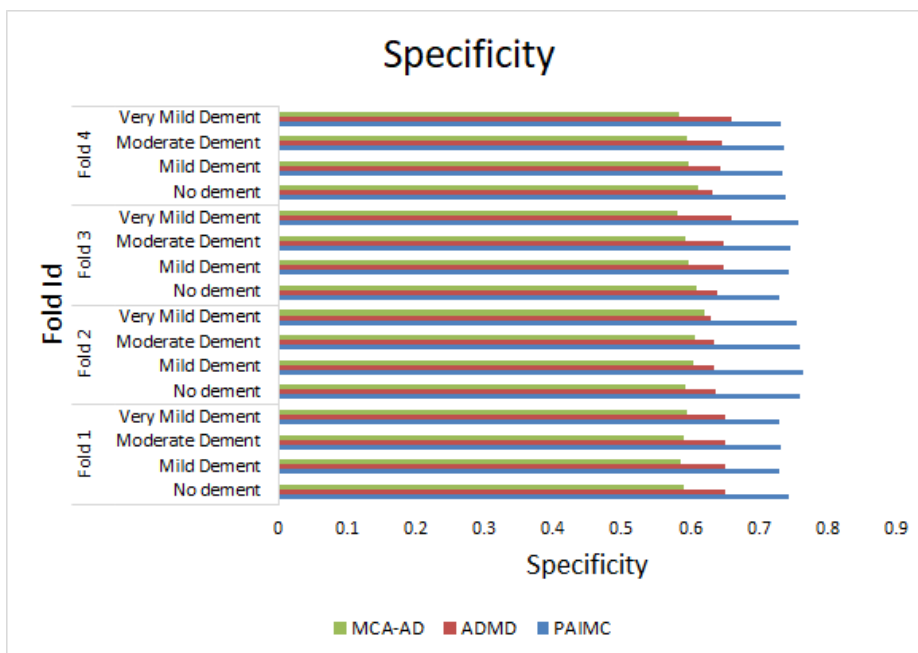
**Figure 8.** Specificity observed for the proposed and models chosen for comparison
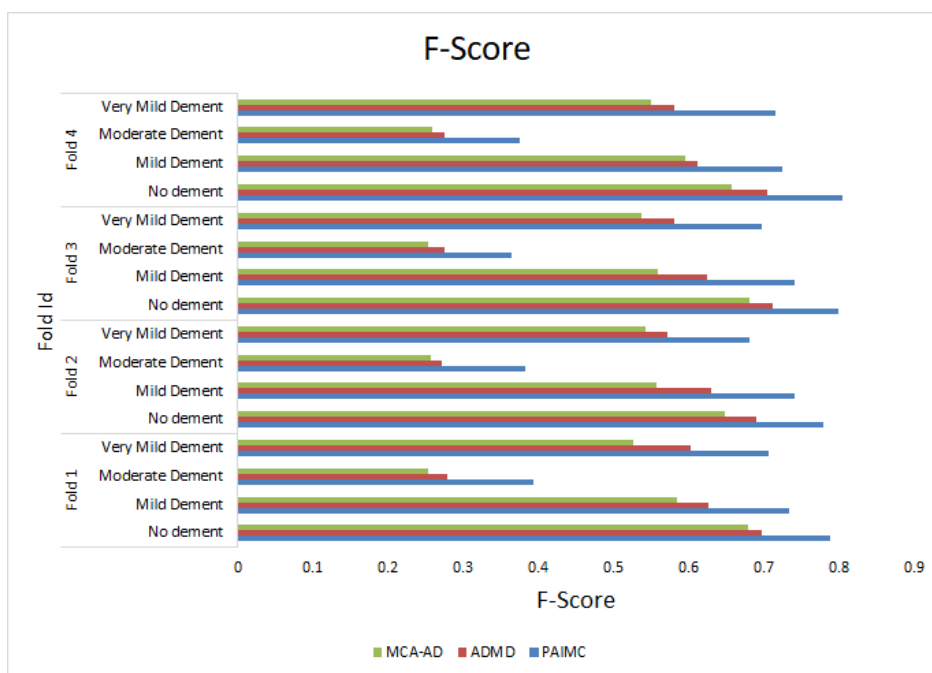


**Figure 9.** Graph showing metric f-score of PAIMC compared to ADMD and MCA-AD with regard to four-fold cross validation.

In figure 6, the performance of the projected approach PAIMC and existing approach MCA-AD and ADMD have been compared by using the metric precision at different labels called No dement, Mild dement, Moderate dement and severe dement over the four folds. It has been envisioned from above statistics that, the performance of the projected model PAIMC performs much more superior at all the labels when compared to existing models.

In figure 7, the performance of the projected approach PAIMC and existing approach MCA-AD and ADMD have been compared by using the metric sensitivity at different labels called No dement, Mild dement, Moderate dement and severe dement over the four folds. It has been envisioned from above statistics that, the performance of the projected model PAIMC performs much more superior at all the labels when compared to existing models.

The ratio determined for real negatives among the total number of actual negatives taken into account is one of the essential measurements, and it is highlighted in Figure 8 with a focus on specificity factors. The suggested model, PAIMC, performs better than the other two important models, MCA-AD and ADMD, when compared to the test dataset, as seen in the graphical depiction of performance according to the criteria.

In figure 9, the performance of the projected approach PAIMC and existing approach MCA-AD and ADMD have been compared by using the metric F-measure at different labels called No dement, Mild dement, Moderate dement and severe dement over the four folds. It has been envisioned from above statistics that, the performance of the projected model PAIMC performs much more superior at all the labels when compared to existing models.

In figure 10, the performance of the projected approach PAIMC and existing approach MCA-AD and ADMD have been compared by using the metric Accuracy at different labels called No dement, Mild dement, Moderate dement and severe dement over the four folds. It has been envisioned from above statistics that, the performance of the projected model PAIMC performs much more superior at all the labels when compared to existing models.



**Figure 10.** Graphical representation of comparison of proposed model PAIMC and contemporary model's ADMD and MCA-AD in terms of metric Accuracy over four folds.
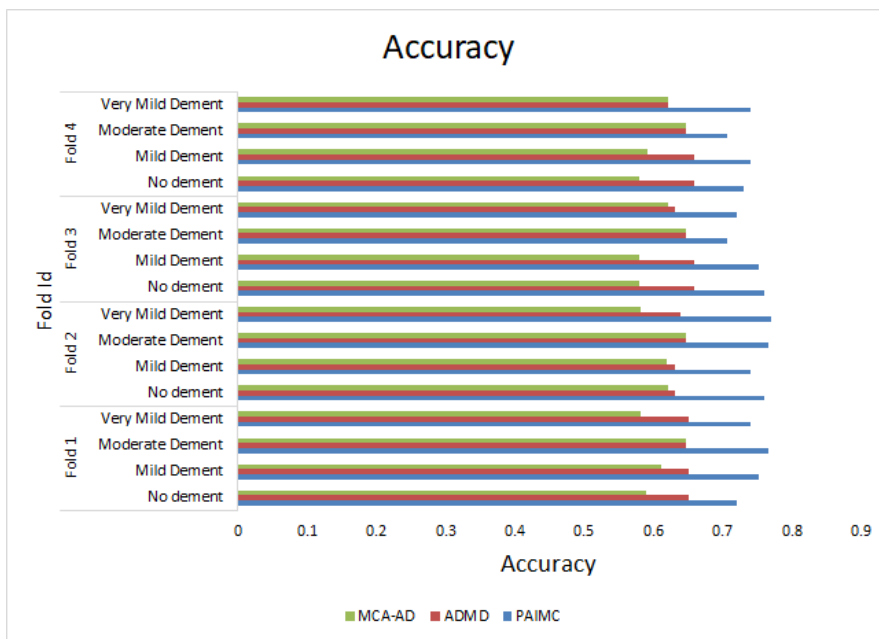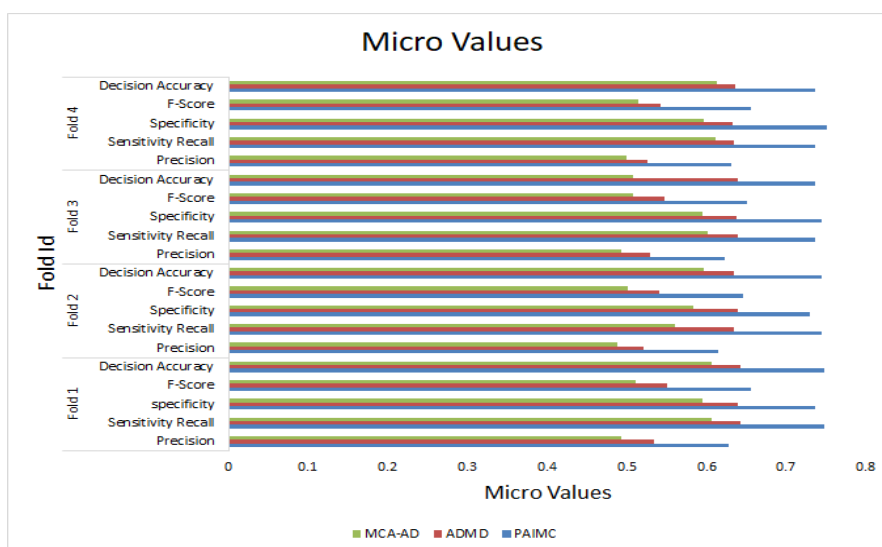


**Figure 11.** Graph showing micro values of all metrics of PAIMC compared to ADMD and MCA-AD with regard to four-fold cross validation.

Figure 11 illustrates the metrics for the predicted model PAIMC and the current models MCA-AD and ADMD through the four folds. These metrics include precision, F-score, decision accuracy, and sensitivity. The proposed model is expected to outperform existing metrics in every statistic when compared to them.

## 5. Conclusion

This manuscript has demonstrated an ensemble classification model adept at distinguishing between various stages of Alzheimer's disease—mild dementia, no dementia, moderate dementia, and very mild dementia—utilizing MRI data from diverse subjects. Through a rigorous four-fold multi-label cross-validation process, it has been established that our proposed model, PAIMC, surpasses the current benchmarks set by models such as ADMD and MCA-AD in terms of accuracy and reliability.

Looking ahead, future research endeavors could focus on integrating evolutionary algorithms to further refine feature optimization, enhancing the model's ability to discern subtle differences between the disease stages. Additionally, the exploration of unsupervised learning techniques presents a promising avenue for dividing the training data more effectively, thereby addressing the challenge of high dimensionality in the data. This approach could lead to notable improvements in the ensemble model's decision accuracy. Furthermore, investigating the application of deep learning architectures may uncover patterns within the data that traditional machine learning methods might overlook, potentially leading to breakthroughs in early detection and classification of Alzheimer's disease. The incorporation of longitudinal study designs could also provide insights into the progression of the disease, enabling more dynamic and predictive modeling. These advancements could significantly contribute to the precision and utility of diagnostic tools, ultimately aiding in the development of personalized treatment plans and interventions for Alzheimer's disease.

## References

[1]     R.J. Harvey, M. Skelton-Robinson, M.N. Rossor, The prevalence and causes of dementia in people under the age of 65 years. Journal Neurology, Neurosurgery & Psychiatry, 74(9), (2003) 1206-1209. https://doi.org/10.1136/jnnp.74.9.1206

[2]     M. Prince, A. Comas-Herrera, M. Knapp, M. Guerchet, M. Karagiannidou, World Alzheimer report 2016: improving healthcare for people living with dementia: coverage, quality and costs now and in the future. Alzheimer's disease International (ADI), London, UK.

[3]     A. McMurtray, D.G. Clark, D. Christine, M.F. Mendez, Early-onset dementia: frequency and causes compared to late-onset dementia. Dementia and Geriatric Cognitive Disorders, 21(2), (2006) 59-64. https://doi.org/10.1159/000089546

[4]     V. Hosamani, H.S. Vimala, Data Science: Prediction and Analysis of Data using Multiple Classifier System, International Journal of Computer Engineering in Research Trends, 5(12), (2018) 216–222. https://doi.org/10.22362/ijcert/2018/v5/i12/v5i1201

[5]     C. Eckerström, E. Olsson, M. Borga, S. Ekholm, S. Ribbelin, S. Rolstad, G. Starck, Å. Edman, A. Wallin, H. Malmgren, Small baseline volume of left hippocampus is associated with subsequent conversion of MCI into dementia: the Göteborg MCI study. Journal Neurological Sciences, 272(1-2), (2008) 48-59. https://doi.org/10.1016/j.jns.2008.04.024

[6]     D. Facal, S. Valladares-Rodriguez, C. Lojo-Seoane, A.X. Pereiro, L. Anido-Rifon, O. Juncos-Rabadán, Machine learning approaches to studying the role of cognitive reserve in conversion from mild cognitive impairment to dementia. International journal of geriatric psychiatry, 34(7), (2019) 941-949. https://doi.org/10.1002/gps.5090

[7]     A.M. Darcy, A.K. Louie, L.W. Roberts, Machine learning and the profession of medicine. Jama, Network, 315(6) (2016) 551-552. https://doi.org/10.1001/jama.2015.18421

[8]     M. Prince, E. Albanese, M. Guerchet, M. Prina, World Alzheimer Report 2014: Dementia and risk reduction: An analysis of protective and modifiable risk factors. HAL.

[9]     A.A. Ibrahim, A. Alhialy, Enhancing Diabetes Risk Assessment in PIMA Indians: A Machine Learning Approach Using AdaBoost. International Journal of Computer Engineering in Research Trends, 10(6), (2023) 15–21. https://doi.org/10.22362/ijcert/2023/v10/i06/v10i0603

[10]    Alzheimer's Association, 2014 Alzheimer's disease facts and figures. Alzheimer's & Dementia, 10(2), (2014) e47-e92. https://doi.org/10.1016/j.jalz.2014.02.001

[11]    K.G. Yiannopoulou, S.G. Papageorgiou, Current and future treatments for Alzheimer's disease. Therapeutic Advances in Neurological Disorders, 6, (2013) 19-33. https://doi.org/10.1177/1756285612461679

[12]    D. Zhang, D. Shen, Alzheimer's Disease Neuroimaging Initiative, Predicting future clinical changes of MCI patients using longitudinal and multimodal biomarkers. PloS one. 7(3), (2012) e33182. https://doi.org/10.1371/journal.pone.0033182

[13]    A. Nordberg, J.O. Rinne, A. Kadir, B. Langstrom,

The use of PET in Alzheimer disease. Nature Reviews Neurology, 6(2), (2010) 78-87. https://doi.org/10.1038/nrneurol.2009.217

[14] H.I. Suk, C.Y. Wee, D. Shen, Discriminative group sparse representation for mild cognitive impairment classification. International Workshop on Machine Learning in Medical Imaging, Springer, Cham, (2013) 131-138. https://doi.org/10.1007/978-3-319-02267-3_17

[15] S. Keihaninejad, H. Zhang, N.S. Ryan, I.B. Malone, M. Modat, M. Jorge Cardoso, D.M. Cash, N.C. Fox, S. Ourselin, An unbiased longitudinal analysis framework for tracking white matter changes using diffusion tensor imaging with application to Alzheimer's disease. Neuroimage, 72, (2013) 153-163. https://doi.org/10.1016/j.neuroimage.2013.01.044

[16] T. Tong, R. Wolz, Q.Gao, R. Guerrero, J.V. Hajnal, D. Rueckert, the Alzheimer's Disease Neuroimaging Initiative, Multiple instance learning for classification of dementia in brain MRI. Medical Image Analysis, 18(15), (2014) 808-818. https://doi.org/10.1016/j.media.2014.04.006

[17] M. Goryawala, Q. Zhou, W. Barker, D.A. Loewenstein, R. Duara, M. Adjouadi, Inclusion of neuropsychological scores in atrophy models improves diagnostic classification of Alzheimer's disease and mild cognitive impairment. Computational intelligence and neuroscience, 2015, (2015). https://doi.org/10.1155/2015/865265

[18] E. Janoušová, M. Vounou, R. Wolz, K.R. Gray, D. Rueckert, G. Montana, (2012) Biomarker discovery for sparse classification of brain images in Alzheimer's disease. Annals of the BMVA, 2.

[19] S.F. Eskildsen, P. Coupe, D. García-Lorenzo, V. Fonov, J.C. Pruessner, D.L. Collins, & Alzheimer's Disease Neuroimaging Initiative, Prediction of Alzheimer's disease in subjects with mild cognitive impairment from the ADNI cohort using patterns of cortical thinning," Neuroimage, 65 (2013) 511-521. https://doi.org/10.1016/j.neuroimage.2012.09.058

[20] N.M. Patil, M.U. Nemade, Music genre classification using MFCC, K-NN and SVM classifier. International Journal of Computer Engineering in Research Trends, 4(2), (2017) 43-47.

[21] J.Y. Tou, Y.H. Tay, P.Y. Lau, (2008) One-dimensional grey-level co-occurrence matrices for texture classification. International Symposium on Information Technology, Malaysia. https://doi.org/10.1109/ITSIM.2008.4631992

[22] G.W. Jiji, G.E. Suji, M. Rangini, An intelligent technique for detecting Alzheimer's disease based on brain structural changes and hippocampal shape. Computer Methods in Biomechanics and Biomedical Engineering: Imaging & Visualization, 2(2), (2014) 121-128. https://doi.org/10.1080/21681163.2013.879838

[23] M.S. De Oliveira, M.L.F. Balthazar, A. D'abreu, C.L. Yasuda, B.P. Damasceno, F. Cendes, & G. Castellano, MR imaging texture analysis of the corpus callosum and thalamus in amnestic mild cognitive impairment and mild Alzheimer disease. American Journal of Neuroradiology, 32(1), (2011) 60-66. https://doi.org/10.3174/ajnr.A2232

[24] M. Torabi, R.D. Ardekani, E. Fatemizadeh, (2006) Discrimination between Alzheimer's disease and control group in MR-images based on texture analysis using artificial neural network International Conference on Biomedical and Pharmaceutical Engineering, Singapore.

[25] P. Ghorbanian, D.M. Devilbiss, A. Verma, A. Bernstein, T. Hess, A.J. Simon, H. Ashrafiuon, Identification of resting and active state EEG features of Alzheimer's disease using discrete wavelet transform. Annals of biomedical engineering, 41, (2013) 1243-1257. https://doi.org/10.1007/s10439-013-0795-5

[26] P.B. Abhi, K.A.R. Torres, T. Yusoff, K. Samunnisa, A Novel Lightweight Cryptographic Protocol for Securing IoT Devices. International Journal of Computer Engineering in Research Trends, 10, (2023) 24-30.

[27] Y. Guo, Z. Zhang, B. Zhou, P. Wang, H. Yao, M. Yuan, N. An, H. Dai, L. Wang, X. Zhang & Y. Liu, Grey-matter volume as a potential feature for the classification of Alzheimer's disease and mild cognitive impairment: an exploratory study. Neuroscience bulletin, 30, (2014) 477-489. https://doi.org/10.1007/s12264-013-1432-x

[28] A. M. Martinez, A.C. Kak, PCA versus LDA. IEEE Transactions on Pattern Analysis and Machine Intelligence, 23(2), (2001) 228-233. https://doi.org/10.1109/34.908974

[29] D. Salas-Gonzalez, J.M. Górriz, J. Ramírez, M. López, I. Álvarez, F. Segovia, C.G. Puntonet, Computer-aided diagnosis of Alzheimer's disease using support vector machines and classification trees. Physics in Medicine & Biology, 55(10), (2010) 2807. https://doi.org/10.1088/0031-9155/55/10/002

[30] O. Yamashita, Masa-aki Sato, Taku Yoshioka, Frank Tong, Yukiyasu Kamitani, Sparse estimation automatically selects voxels relevant for the decoding of fMRI activity patterns. Neuroimage, 42(4), (2008) 1414-1429. https://doi.org/10.1016/j.neuroimage.2008.05.050

[31] P. Pradeep, J. Kamalakannan, Effective Predictor Model for Parkinson's Disease Using

Machine Learning. International Journal of Computer Engineering in Research Trends, 10(4), (2023) 204–209. https://doi.org/10.22362/ijcert/2023/v10/i04/v10i0410

[32] S.J. Hanson, Y.O. Halchenko, and Brain reading using full brain support vector machines for object recognition: there is no 'face' identification area. Neural Computation, 20(2), (2008) 486-503. https://doi.org/10.1162/neco.2007.09-06-340

[33] C. Chu, A.L. Hsu, K.H. Chou, P. Bandettini, C. Lin, Alzheimer's Disease Neuroimaging Initiative, Does feature selection improve classification accuracy? Impact of sample size and feature selection on classification using anatomical magnetic resonance images. Neuroimage, 60(1), (2012) 59-70. https://doi.org/10.1016/j.neuroimage.2011.11.066

[34] A.R. Hidalgo-Muñoz, M.M. López, I.M. Santos, A.T. Pereira, M. Vázquez-Marrufo, A. Galvao-Carmona, A.M. Tomé,. Application of SVM-RFE on EEG signals for detecting the most relevant scalp regions linked to affective valence processing. Expert systems with Applications, 40(6), (2013) 2102-2108. https://doi.org/10.1016/j.eswa.2012.10.013

[35] A.R. Hidalgo-Muñoz, J. Ramírez, J.M. Górriz, & P. Padilla, Regions of interest computed by SVM wrapped method for Alzheimer's disease examination from segmented MRI. Frontiers in aging neuroscience, 6, (2014) 20. https://doi.org/10.3389/fnagi.2014.00020

[36] M. Gönen, E. Alpaydın, Multiple kernel learning algorithms. The Journal of Machine Learning Research, 12, (2011) 2211-2268.

[37] O.B. Ahmed, J. Benois-Pineau, M. Allard, G. Catheline, C.B. Amar, & Alzheimer's Disease Neuroimaging Initiative.. Recognition of Alzheimer's disease and Mild Cognitive Impairment with multimodal image-derived biomarkers and Multiple Kernel Learning. Neurocomputing, 220(12), (2017) 98-110. https://doi.org/10.1016/j.neucom.2016.08.041

[38] K.R. Kruthika, H.D. Maheshappa, Alzheimer's Disease Neuroimaging Initiative. Multistage classifier-based approach for Alzheimer's disease prediction and retrieval. Informatics in Medicine Unlocked, 14, (2019) 34-42. https://doi.org/10.1016/j.imu.2018.12.003

[39] R. Ju, C. Hu, Q. Li, Early diagnosis of Alzheimer's disease based on resting-state brain networks and deep learning. IEEE/ACM Transactions on Computational Biology and Bioinformatics, 16(1), (2017) 244-257. https://doi.org/10.1109/TCBB.2017.2776910

[40] R. Cui, M. Liu, Alzheimer's Disease Neuroimaging Initiative, RNN-based longitudinal analysis for diagnosis of Alzheimer's disease. Computerized Medical Imaging and Graphics, 73, (2019) 1-10. https://doi.org/10.1016/j.compmedimag.2019.01.005

[41] V. Karami, F. Amenta, G. Noce, C. Del Percio, R. Lizio, M.T. Pascarelli, M. Blūma, C. Babiloni, P68-F Abnormalities of cortical neural synchronization mechanisms in patients with Alzheimer's diseases dementia: An EEG studyClinical Neurophysiology, 130(7), (2019) e86-e87. https://doi.org/10.1016/j.clinph.2019.04.517

[42] F. Er, P. Iscen, S. Sahin, N. Cinar, S. Karsidag, D. Goularas, Distinguishing age-related cognitive decline from dementias: A study based on machine learning algorithms. Journal of Clinical Neuroscience, 42, (2017) 186-192. https://doi.org/10.1016/j.jocn.2017.03.021

[43] C.R. Aditya, M.S. Pande, Devising an interpretable calibrated scale to quantitatively assess the dementia stage of subjects with Alzheimer's disease: A machine learning approach. Informatics in Medicine Unlocked, 6, (2017) 28-35. https://doi.org/10.1016/j.imu.2016.12.004

[44] L. Liu, S. Zhao, H. Chen, A. Wang, A new machine learning method for identifying Alzheimer's disease. Simulation Modelling Practice and Theory, 99, (2020) 102023. https://doi.org/10.1016/j.simpat.2019.102023

[45] G. Battineni, N. Chintalapudi, F. Amenta, Machine learning in medicine: Performance calculation of dementia prediction by support vector machines (SVM). Informatics in Medicine Unlocked, 16, (2019) 100200. https://doi.org/10.1016/j.imu.2019.100200

[46] C. Jimenez-Mesa, I.A. Illán, A. Martin-Martin, D. Castillo-Barnes, F.J. Martinez-Murcia, J. Ramirez, J.M. Gorriz, Optimized one vs one approach in multiclass classification for early Alzheimer's disease and mild cognitive impairment diagnosis. IEEE Access, 8, (2020) 96981-96993. https://doi.org/10.1109/ACCESS.2020.2997736

[47] W. Lin, Q. Gao, M. Du, W. Chen, T. Tong, Multiclass diagnosis of stages of Alzheimer's disease using linear discriminant analysis scoring for multimodal data. Computers in Biology and Medicine, 134, (2021) 104478. https://doi.org/10.1016/j.compbiomed.2021.104478

[48] C.H. Lai, S.S. Yu, H.Y. Tseng, & M.H. Tsai, A protozoan parasite extraction scheme for digital microscopic images. Computerized Medical Imaging and Graphics, 34(2), (2010) 122-130. https://doi.org/10.1016/j.compmedimag.2009.07.008

[49] R.C. Gonzalez, R.E. Woods, & S.L. Eddins, (2004) Digital image processing using MATLAB,

Pearson Education India.

[50] A.P.S. Pharwaha, B. Singh, Shannon and non-shannon measures of entropy for statistical texture feature extraction in digitized mammograms. In Proceedings of the world congress on engineering and computer science, 2(6), (2009) 20-22.

[51] M. Ghosh, D. Das, & C. Chakraborty, (2010) Entropy based divergence for leukocyte image segmentation. In 2010 International Conference on Systems in Medicine and Biology, IEEE, India. https://doi.org/10.1109/ICSMB.2010.5735414

[52] F.B. Tek, A.G. Dempster, I. Kale, Computer vision for microscopy diagnosis of malaria. Malaria journal, 8, (2009) 1-14. https://doi.org/10.1186/1475-2875-8-153

[53] F.B. Tek, A.G. Dempster, I. Kale, Parasite detection and identification for automated thin blood film malaria diagnosis. Computer vision and image understanding, 114(1), (2010) 21-32. https://doi.org/10.1016/j.cviu.2009.08.003

[54] M.M. Galloway, Texture classification using gray level run length. Computer Graphics and Image Processing. 4(2), (1975) 172-179. https://doi.org/10.1016/S0146-664X(75)80008-6

[55] A. Chu, C.M. Sehgal, J.F. Greenleaf, Use of gray value distribution of run lengths for texture analysis. Pattern recognition letters, 11(6), (1990) 415-419. https://doi.org/10.1016/0167-8655(90)90112-F

[56] B.V. Dasarathy, E.B. Holder, Image characterizations based on joint gray level-run length distributions. Pattern Recognition Letters, 12(8), (1991) 497-502. https://doi.org/10.1016/0167-8655(91)80014-2

[57] M. Muthu Rama Krishnan, P. Shah, C. Chakraborty, & A.K. Ray, Statistical analysis of textural features for improved classification of oral histopathological images. Journal of medical systems, 36, (2012) 865-881. https://doi.org/10.1007/s10916-010-9550-8

[58] B.B. Mandelbrot, (1983) the fractal geometry of nature/Revised and enlarged edition. Freeman and Co, New York.

[59] N. Sarkar, B.B. Chaudhuri, An efficient differential box-counting approach to compute fractal dimension of image. IEEE Transactions on Systems, Man, and Cybernetics, 24(1), (1994) 115-120. https://doi.org/10.1109/21.259692

[60] T. Ojala, M. Pietikainen, T. Maenpaa, Multiresolution gray-scale and rotation invariant texture classification with local binary patterns. IEEE Transactions on Pattern Analysis and Machine Intelligence, 24(7), (2002) 971-987. https://doi.org/10.1109/TPAMI.2002.1017623

[61] M.M. Krishnan, Textural characterization of histopathological images for oral sub-mucous fibrosis detection. Tissue and Cell, 43(5), (2011) 318-330. https://doi.org/10.1016/j.tice.2011.06.005

[62] M.K. Hu, Visual pattern recognition by moment invariants. IRE Transactions on Information Theory, 8(2), (1962) 179-187. https://doi.org/10.1109/TIT.1962.1057692

[63] D. Das, M. Ghosh, C. Chakraborty, M. Pal, A.K. Maity, (2010) Invariant moment-based feature analysis for abnormal erythrocyte recognition. In 2010 International conference on systems in medicine and biology, IEEE, India. https://doi.org/10.1109/ICSMB.2010.5735380

[64] I. Guyon, A. Elisseeff, An introduction to variable and feature selection. Journal of machine learning research, 3, (2003) 1157-1182.

[65] H. Budak, S.E. Taşabat, A modified t-score for feature selection. Anadolu University Journal of Science and Technology A - Applied Sciences and Engineering, 17(6), (2016) 845-852. https://doi.org/10.18038/aubtda.279853

[66] T. Naga Lakshmi, S. Jyothi, M. Rudra Kumar, Image Encryption Algorithms Using Machine Learning and Deep Learning Techniques-A Survey. in Modern Approaches in Machine Learning and Cognitive Science: A Walkthrough, Springer, (2021) 507-515. https://doi.org/10.1007/978-3-030-68291-0_40

[67] M. Rudra Kumar, V.K. Gunjan, (2022) Peer Level Credit Rating: An Extended Plugin for Credit Scoring Framework. in ICCCE 2021, Lecture Notes in Electrical Engineering, 828, Springer, Singapore, https://doi.org/10.1007/978-981-16-7985-8_128

[68] O.K.J. Savoy, Feature selection in sentiment analysis. In Proceedings of the 9th French Information Retrieval Conference, (2012) 273-284.

[69] P. Sahoo, T. Riedel, (1998) Mean value theorems and functional equations. World Scientific. https://doi.org/10.1142/3857

[70] J.R. Dwaram, M. Rudra Kumar, Crop yield forecasting by long short-term memory network with Adam optimizer and Huber loss function in Andhra Pradesh, India. Concurrency and Computation Practice Experience, 34(27), (2022) e7310. https://doi.org/10.1002/cpe.7310

[71] M.S. Thulasi, B. Sowjanya, K. Sreenivasulu, M.R. Kumar, Knowledge attitude and practices of dental students and dental practitioners towards artificial intelligence. International Journal of Intelligent Systems and Applications in Engineering, 10(1), (2022) 248-253.

[72] B. Burt Gerstman, "t-Table," San Jose State University, (2017). [Online]. Available at: http://www.sjsu.edu/faculty/gerstman/StatPrimer/t-table.pdf

[73]   R. Real, J.M. Vargas, The probabilistic basis of Jaccard's index of similarity, Systematic Biology, 45(3), (1996) 380-385. https://doi.org/10.1093/sysbio/45.3.380

[74]   T. Kent, Information gain and a general measure of correlation. Biometrika, 70(1), (1983) 163-173. https://doi.org/10.1093/biomet/70.1.163

**Authors Contribution Statement**

P. Radhika Raju - Conceptualization, Methodology, data collection, formal analysis, Writing - Original Draft, Writing - Review & Editing. A. Ananda Rao - Conceptualization, Methodology, Writing - Original Draft, Writing - Review & Editing. Both authors have approved the final version of the manuscript and agree to be accountable for all aspects of the work.

**Data Availability**

Data generated during the study will be made available on reasonable request.

**Conflict of Interest**

The Authors confirm there's aren't any competing interests with respect towards this paper's release.

**Has this article screened for similarity?**

Yes

**About the License**